Proceedings of the 9th International Symposium on Fluid-Structure Interactions, Flow-Sound Interactions, Flow-Induced Vibration & Noise
July 8-11, 2018, Toronto, Ontario, Canada

FIV2018-46

A FIXED-GRID FLUID STRUCTURE INTERACTION METHOD FOR FULLY-COUPLED COMPRESSIBLE SOLID AND INCOMPRESSIBLE FLUID

Song Yu
Institute of Nuclear and New Energy Technology, Tsinghua University, Beijing 100084, China
Collaborative Innovation Center of Advanced Nuclear Energy Technology
Key Laboratory of Advanced Reactor Engineering and Safety, Ministry of Education of China

Zhao Jiaqing
Institute of Nuclear and New Energy Technology, Tsinghua University, Beijing 100084, China
Collaborative Innovation Center of Advanced Nuclear Energy Technology
Key Laboratory of Advanced Reactor Engineering and Safety, Ministry of Education of China

Tan Lei
State Key Laboratory of Hydroscience and Engineering, Tsinghua University, Beijing 100084, China

Cao Shuliang
State Key Laboratory of Hydroscience and Engineering, Tsinghua University, Beijing 100084, China

ABSTRACT
In this paper, we develop a fixed-grid fluid-structure interaction method - immersed volume method to solve the fluid structure interaction problem. In this method, the fluid mesh exists in the whole fluid and solid domain, and the solid is regarded as real occupation overlap the fluid domain. The fluid equations are solved in the whole FSI domain. While the fluid and solid interaction conditions are only transmitted on the fluid-structure interface. The proposed method avoids the interaction of the fluid and solid velocity except on the fluid-structure interface and has strong ability to solve the FSI problems for the compressible solid and the incompressible fluid. A 2D flow passing and elastic wall problem is simulated using the IVM. The solid deformation and fluid pressure variation shows good agreement with the traditional Arbitrary Lagrangian Eulerian method. A rotating rotor in a cavity is then computed to testify the robust of the boundary tracking scheme.

INTRODUCTION
Fluid-structure interaction (FSI) is a crucial consideration in the design of many engineering systems problems, e.g. hydraulic machinery, nuclear equipment. The main challenge to solve these problems arises from their strong nonlinearity and multidisciplinary nature. For most FSI problems, analytical solutions to the governing equations are impossible to obtain, whereas laboratory experiments are limited in scope. Therefore, to investigate the fundamental physics involved in the complex interaction between fluids and solids, numerical method plays an important role.

In the past few decades, numerous works has been done to develop more robust and efficient techniques to simulate the FSI problems.A general classification of the FSI solution procedures is based upon the mathematically treatment of meshes: the conforming mesh methods and non-conforming mesh methods. The conforming mesh methods are commonly applied to solve the coupling issues with simple physical meanings, such as the Arbitrary Lagrangian Eulerian (ALE) approach [1, 2]. In this approach, the fluid and solid computational domain are separated by the fluid-structure interface, where the information is communicated. As the solid deforming with time, the fluid computational domain varies, when re-meshing is inevitable. The conforming mesh approach could integrate available disciplinary algorithms which have been validated and used for solving many complicated fluid or structural problems. However, the re-meshing process in each time step is computational expensive and could cause distorted mesh or even divergence results when the solid suffers large deformation. The non-conforming mesh method is developed to overcome the above problem. The most prominent non-

conforming mesh methods are the immersed boundary method [3] and its derivations [4, 5]. In these method, the solid and fluid mesh are overlapped and the fluid mesh points do not conform to the fluid-solid interface. The interaction equilibrium is achieved by interface schemes on the non-conforming mesh points around the fluid-structure interface, the precision of which greatly affects the precision of the whole FSI method generally. As a result, the fluid and solid equations can be solved independently with their respective grids all the time, and re-meshing is not necessary. However, the immersed boundary method assumes the solid domain as a fiber-like material, whose physical properties, such as Young's modulus and volume, could not be considered. This assumption limits the application of the method in certain fields [6] including biology problems in which the fluid and solid share the similar properties, flows with suspended particles, and flows past a fixed boundary cylinder, etc. Wang *et al*. [7] and Zhang *et al*. [8] extended the immersed boundary method to the immersed finite element method (IFEM), in which they considered the solid as an occupied volume immersed in the fluid domain. The effect of the immersed solid was represented by the equivalent nodal forces applied on the fluid particles in the immersed domain. The fluid and solid velocities were assumed to be the same in the immersed domain which is transformed by the delta function of reproducing kernel particle method [9]. Liu *et al*. [10] studied the fluid-structure interaction problems in human cardiovascular systems by using the IFEM. The monocyte and platelet deposition were studied and some preliminary results were presented. Sylvain [11] applied this method to solve the electroencephalography forward problem in order to avoid generating geometry fitting mesh. Gay *et al*. [12] simulated the motion of stent during and after implantation. Lee *et al*. [13, 14] used the transformed finite element basis function to replace delta function to narrow the influence domain near the fluid-structure interface. Thomas *et al*. [15] proposed an integral equation formulation to enforce essential boundary condition in the IFEM.

However, in the IFEM, the velocity of solid is equal to the fluid velocity at the same position in the immersed domain. The assumption is reasonable when the fluid and solid domains share the similar physical properties. Nevertheless, in most FSI problems, the physical properties, e.g. the compressibility, of the fluid and solid are quite different [8, 12]. For this kind of FSI problems, the IFEM could not properly reveal the structure response affected by the surrounding fluid. Therefore, this assumption will prevent the IFEM method from solving the incompressible fluid and compressible solid coupling problems. Wang *et al*. [16] develop a modified immersed finite element method later. In this method, they capture the solid dynamic by solving the solid governing equation instead of calculated from the fluid velocities. This is a big improvement to let the solid behave as solid. However, they make the artificial fluid domain behave like solid as much as possible by enforcing the fluid velocity equal to the solid velocity in the immersed domain using delta function. This assumption makes it easy to satisfy the fluid-structure boundary condition. While, this assumption could bring in big error in the pressure field near the solid.

In the present paper, the immersed volume method (IVM) is originally developed to solve the incompressible fluid and compressible solid coupling problems. The IVM introduces the independent fictitious fluid particles under the solid domain mathematically to distinguish the different compressible behavior of the fluid and solid. A new boundary tracking scheme guarantees that only real fluid particles are related to the interface equilibrium with more clear physical meaning. The flow passing an elastic wall case is analyzed using present method and ALE method respectively. The performance of the present method is verified by comparing the solid deformation and flow distribution with ALE method. The stirring rotor in a cavity case is then simulated to verify the robustness of the boundary tracking scheme.

GOVERNING EQUATIONS

Figure 1 shows the description of compressible solid and incompressible fluid interaction problem, where Ω is the entire domain, Ω_s is the solid domain, Ω_f is the physical fluid domain, and Γ is the fluid-structure interface. We assume that the fictitious fluid exists under the solid domain which employs only for mathematically calculation without any physical meanings. The velocities of the fictitious fluid are independent of the solid particles on the top.

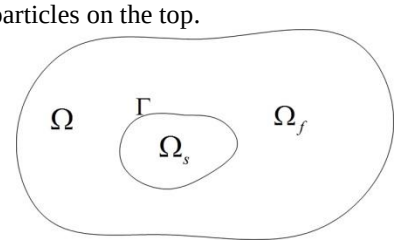

FIGURE 1: DESCRIPTION OF FLUID STRUCTURE INTERACTION PROBLEM.

In the present method, Ω is the fluid computational domain filled with Eulerian mesh, including the physical fluid domain Ω_f and the fictitious fluid domain Ω_s. Ω_s is also the solid computational domain filled with Lagrangian mesh overlapping with Ω.

For a continuum, fluid particles or solid particles, the following equations are satisfied in Ω_f or Ω_s:

$$\rho \frac{dv_i}{dt} = \sigma_{ij,j} + f_i^{ext} \tag{1a}$$

Where ρ is the density, v is the velocity, σ is the Cauchy stress, f^{ext} is the external force, the superscript f and s, denote the fluid and solid particle variables respectively.

For the fictitious fluid particles in Ω_s, The inertial term on the left-hand-side can be decomposed as,

$$\rho^s \frac{dv_i^s}{dt} = \rho^f \frac{dv_i^f}{dt} + (\rho^s \frac{dv_i^s}{dt} - \rho^f \frac{dv_i^f}{dt}) \tag{2}$$

The external force f_i^{ext} is depicted as the gravitational force only, which can be decomposed as,

$$\rho^s g_i = \rho^f g_i + (\rho^s - \rho^f) g_i \tag{3}$$

The derivative of the Cauchy stress can be decomposed as,

$$\sigma^s_{ij,j} = \sigma^f_{ij,j} + \sigma^s_{ij,j} - \sigma^f_{ij,j} \quad (4)$$

According to the above derivation, the governing equations in the whole domain could be written as fluid-like equations with a fluid-structure interaction force FSI_i^f .

$$\rho^f \frac{dv_i^f}{dt} - \sigma^f_{ij,j} = FSI_i^f \quad , \mathbf{x} \in \Omega \quad (5a)$$

$$v^f_{i,i} = 0 \, , \mathbf{x} \in \Omega \quad (5b)$$

$$FSI_i^f = \begin{cases} 0, & \mathbf{x} \in \Omega_f \\ -(\rho^s \frac{dv_i^s}{dt} - \rho^f \frac{dv_i^f}{dt}) + \sigma^s_{ij,j} - \sigma^f_{ij,j} + (\rho^s - \rho^f) g_i \, , & \mathbf{x} \in \Omega_s \end{cases} \quad (5c)$$

Where **x** is the spatial coordinate.

FINITE ELEMENT DISCRETIZATION

Fluid and solid equations

In the proposed method, the conventional fluid and solid computation method could be selected. The updated Lagrangian formulation [17] is implemented to calculated the solid equation.

The Flow-condition-based interpolation (FCBI) finite element procedure [18] is used to solve the incompressible fluid equations. The FCBI finite element method is stable and efficient, and has been widely used in the CFD and FSI [19] fields. Since a continuous pressure distribution is very important to maintain the stability and accuracy of the whole scheme, the 9-node FCBI method is used in the proposed method. The detail derivation of the FCBI finite element method could be found in Ref. [18].

Time integration

To maintain the compatibility of the FSI scheme, the same time integration method is implemented to the fluid and solid equations. For computation simplicity, the first order implicit backward Euler scheme is employed.

Boundary condition

To satisfy the FSI boundary condition on the fluid-structure interface, a mapping scheme between corresponding solid and fluid nodes needs to be developed.

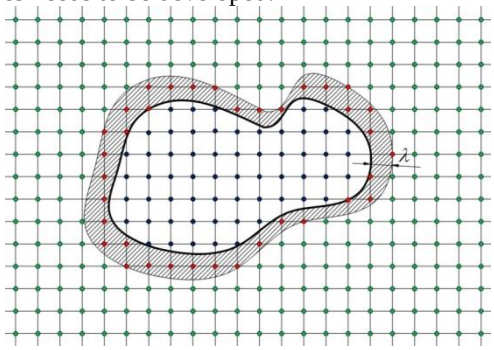

FIGURE 2: COMPUTATIONAL DOMAIN: THE FICTITIOUS FLUID-STRUCTURE INTERFACE (THE RED DOTS); THE FICTITIOUS FLUID NODE (THE BLACK DOTS); THE REAL FLUID NODE (THE GREEN DOTS).

For a given time *t*, as shown in figure 2, Eulerian nodes are divided into three parts: the real fluid part(green points), the fictitious fluid part(black points) and the fictitious fluid-structure interface(red points). The fictitious fluid-structure interface is a set of individual fluid nodes near the real fluid-structure interface (the black thick line). The entire domain is separated into the real fluid part and the fictitious fluid part by the fictitious fluid-structure interface.The criteria to determine the fictitious fluid-structure interface is 1) outside the solid domain with the distance less than a certain value λ 2) the interface is continuous to form an enclosed area 3) only one node exists on the normal direction of the real fluid-structure interface. The shadow area is the set of points the distances of which between 0 and λ away from the fluid-structure interface, where λ is an empirical factor related to the mesh density, which is calculated by the following equation,

$$\lambda = \max\left(\overline{N_1N_2}\cdot\mathbf{n}, \overline{N_1N_3}\cdot\mathbf{n}, \overline{N_1N_4}\cdot\mathbf{n}, \overline{N_2N_3}\cdot\mathbf{n}, \overline{N_2N_4}\cdot\mathbf{n}, \overline{N_3N_4}\cdot\mathbf{n}\right) \quad (6)$$

Where N_1, N_2, N_3, N_4 is the node of the element which contain the fluid-structure interface.

The nodal velocities on the fictitious fluid-structure interface are determined by interpolating the velocities of the particles on the fluid-structure interface and the real fluid particles, which are independent of the fictitious fluid particle.

A second order interpolation scheme [20] is established to compute the velocity on the fictitious fluid-structure interface. As shown in Figure 3, the Node *A* is on the fictitious fluid-structure interface, with velocity $\mathbf{v}_f$ and coordinate (x_f, y_f). Node *M* and Node *N* are the nodes on the fluid-structure interface with the velocity $\mathbf{v}_1$ and $\mathbf{v}_2$, coordinate (x_1, y_1) and (x_2, y_2), respectively. **n** is the normal vector of the interface. Over Point *A*, a line is drew which is parallel to **n**. Node *B* (x_s, y_s) is the pedal of Line *AB* and Line *MN* the coordinate of which satisfies Eq. (7) and (8).

$$y = y_1 + \frac{y_2 - y_1}{x_2 - x_1}(x - x_1) \quad (7)$$

$$\left[(y - y_f),(x - x_f)\right]\cdot\left[(y_2 - y_1),(x_2 - x_1)\right] = 0 \quad (8)$$

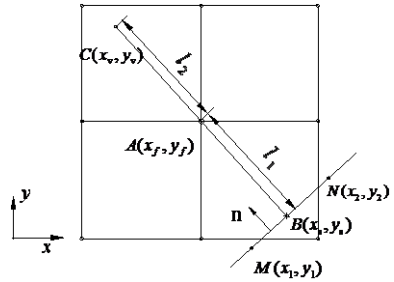

FIGURE 3: INTERPOLATION SCHEME.

The fluid velocity at Node A could be derivied as follows,

Firstly, the virtual Point *C* (x_v, y_v) is determined along *BA* satisfying that l_1=l_2. Since Point *C* is in the real fluid domain, the velocity $\mathbf{v}_v$ at the virtual point C could be identified through linear interpolation in the corresponding element:

$$\mathbf{v}_v = \sum_{i=1,4} h_i \mathbf{v}_{vi} \quad (9)$$

Where $\mathbf{v}_{vi}$ is the nodal velocity of the corresponding element which contains the virtual point. The velocity $\mathbf{v}_s$ of Node *B* is

calculated by linearly interpolating the velocity between Node *M* and Node *N*. The fluid velocity at node *A* could be expressed as the average of the velocities at point *B* and *C*.

VALIDATION EXAMPLES

In order to verify the accuracy and efficacy of the proposed IVM, the result obtained from the IVM is compared with that obtained from the commercial software ADINA, which is verified by many cases [17].

Flow passing an elastic wall

The classical case that flow passing an elastic wall is used to validate the accuracy of the IVM. In this case, 3D problem can be simplified to a 2D model as shown in Figure 4. The whole domain is a 0.02m×0.06m rectangle, and the immersed solid is a 0.01m×0.002m cantilever fixed on the rectangle bottom. The inlet boundary condition is the parabolic velocity with maximum velocity of u_0=0.01m/s, and the outlet is the Neumann boundary condition. Non-slip boundary condition is applied on the cantilever wall. The fluid parameters are ρ_f =1000kg/m^3 and μ=0.001 Pa s. The solid parameters are ρ_s=1025kg/m^3, elasticity modulus E=2×10^6 Pa and Poisson ratio v=0.3. In the present calculation, the solid is considered as compressible and the fluid is considered as incompressible.

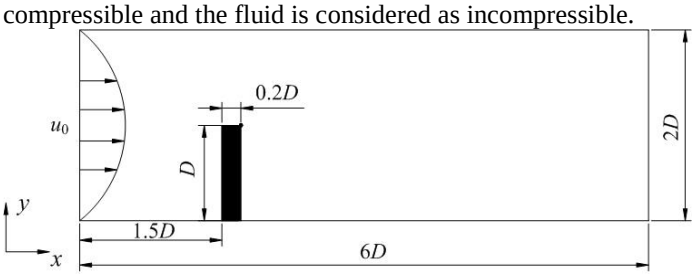

FIGURE 4. FLOW PASSING AN ELASTIC WALL IN 2D.

In the IVM, the whole domain is divided by 9-node quadrilateral Eulerian elements. The overlap solid domain is divided by 9-node quadrilateral Lagrangian elements. In order to verify the grid independence, the problem is analyzed by using four meshes with different densities of 10×30, 20×60, 30×90, 40×120, respectively, and meshes in fluid domain are 6×2, 8×2, 10×2, 12×2, respectively.

The time interval in the present calculation is set as 0.001s. Figure 6 shows the displacement of point *A* at *x* direction at 0.2s calculated by IVM and ADINA respectively. For both IVM and ADINA, when the mesh elements exceed 20×60, the effect of mesh number on calculation result is tiny. Therefore, mesh 20×60 is selected in the following calculation.

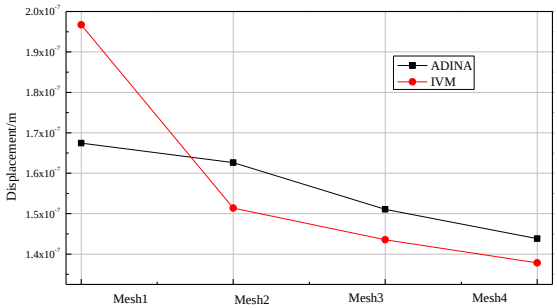

FIGURE 6: DISPLACEMENT OF POINT A AT 0.2S USING DIFFERENT MESH.

Figure 7 shows the configuration of the cantilever at different time with 2000 times magnification for clear display. The cantilever deforms under the fluid impact and the deformation varies with time. The cantilever suffers the largest deformation at about *t*=0.1s. The deformation decreases as the vortex start to form behind the cantilever. The deformation becomes stable at about *t*=1s.

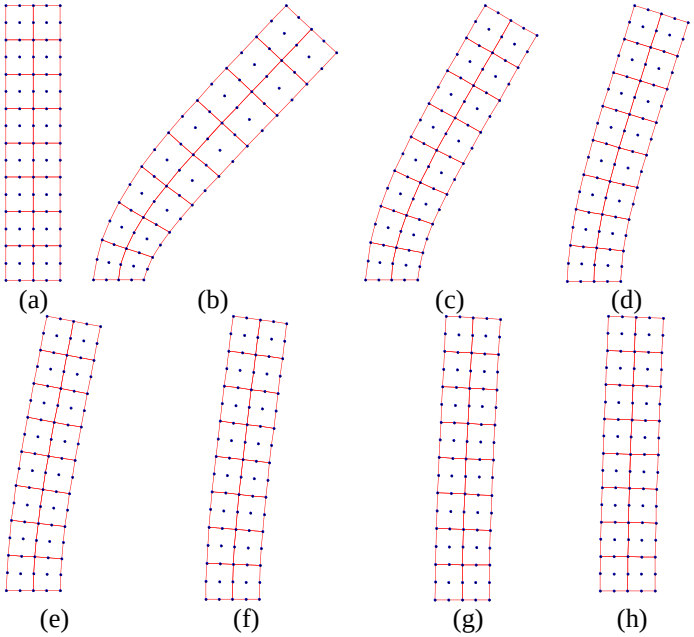

FIGURE 7: CONFIGURATION OF THE CANTILEVER AT DIFFERENT TIME.((a) *t*=0s. (b) *t*=0.1s.(c) *t*=0.2s. (d) *t*=0.3s.(e) *t*=0.4s.(f) *t*=0.5s.(g) *t*=1s.(h) *t*=2s)

Figure 8 shows the pressure distributions of the whole domain at 0.3s, 1s, 2s, 3s, 4s and 5s using the IVM (left) and ADINA (right). As shown in the figure, a vortex incepts near the right-up corner of the cantilever at 0.3s and develops downstream with time. The pressure distribution calculated from IVM agrees well with that from ADINA in the real fluid domain. From the results obtained from the IVM, we observe that the fictitious fluid particles and the real fluid particles share a continuous pressure distribution in the whole domain.

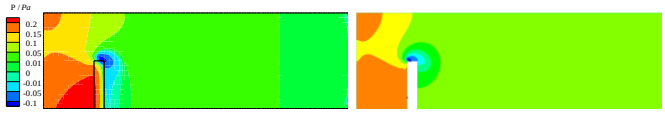

(a) *t*=0.3s

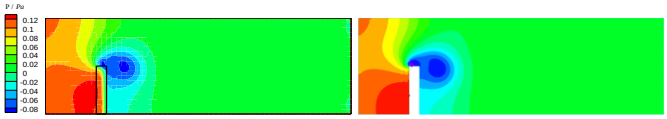

(b) *t*=1.0s

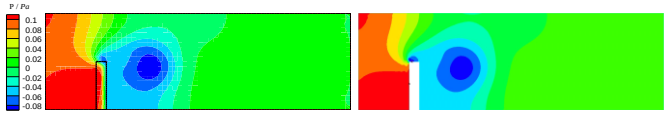

(c) *t*=2.0s

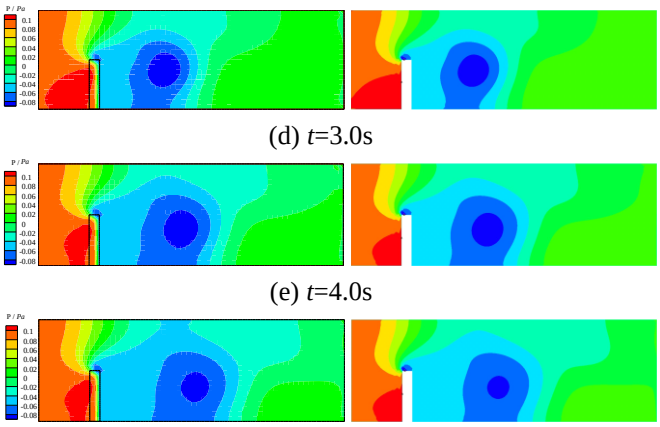

(d) t=3.0s

(e) t=4.0s

(f) t=5.0s

FIGURE 8: TIME EVOLUTION OF PRESSURE DISTRIBUTION FOR IVM (LEFT) AND ADINA (RIGHT).

Rotating rotor in a cavity

A 2D rotating rotor in a cavity is also chosen to verify the IVM method, especially the robustness of the boundary tracking scheme. 2D rotating rotor case is a simplification of the pump impeller in the engineer. Figure 9 shows the geometry domain. Non-slip condition is applied on the cavity left, right and bottom walls and the Neumann condition is imposed on the up wall. The parameters of fluid in the cavity are as follow: ρ_f =1000kg/m^3, μ=0.001 Pa s. The angular velocity of rotating rotor is ω=1 rad/s. The parameters of rotor are as follow: ρ_s=7800kg/m^3, elasticity modulus E=200Gpa and Poisson ratio v=0.3 respectively. While for the IVM, the solid mesh is floating on the fluid mesh, and the re-meshing process can be avoided to save computation time. Especially for the complex solid geometry with irregular deformation, the computation could be quite simplified and great computation time could be saved by avoiding the re-meshing process.

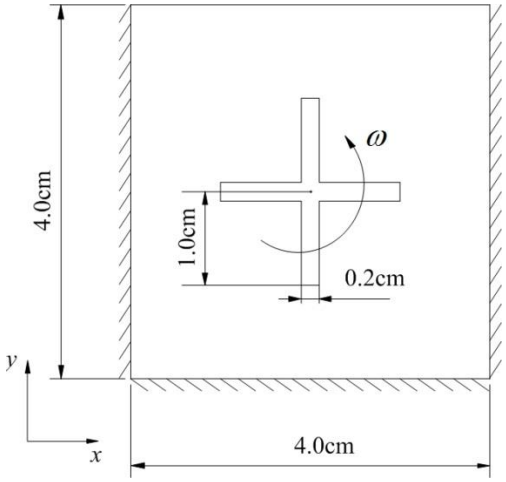

FIGURE 9: GEOMETRY DOMAIN OF ROTATING ROTOR IN A CAVITY.

The fluid domain is divided by 80×80 9-node quadrilateral elements. Solid domain is divided by 9-node quadrilateral elements with element length=0.05cm.

The time step is set as Δt =0.005s, about 1/1256 of the rotating period. Figures 12 and 13 show the pressure and streamline distributions at 0.9s in the whole domain. A pressure concentration near the pressure side of the rotor is detected. The pressure is lower near the suction side of rotor. The streamline of the real fluid domain is shown in Figure13. The pressure and the streamline distribution could clearly describe the interaction between the fluid and solid which reveals the effectiveness of the proposed method.

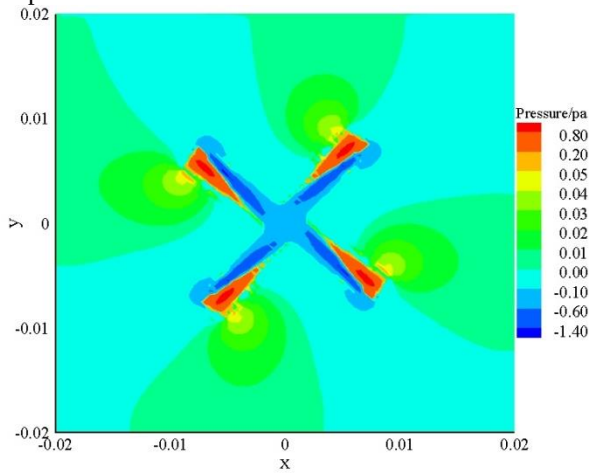

FIGURE 12: PRESSURE DISTRIBUTION IN THE WHOLE DOMAIN.

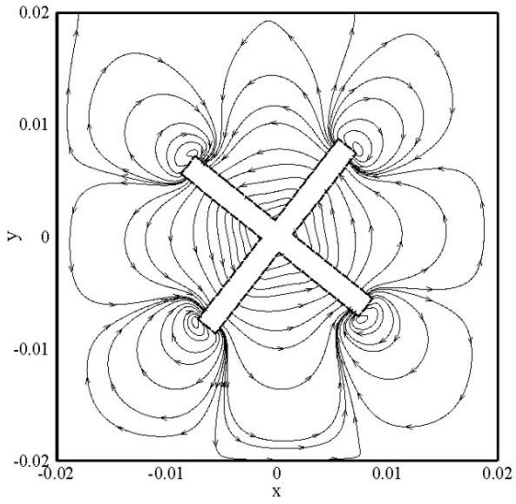

FIGURE 13: STREAMLINES IN THE WHOLE DOMAIN.

When the rotor stirring problem is solved by the ADINA, the fluid domain needs to vary with the solid and a specific algorithm to generate a reasonable mesh at each time step is necessary. Firstly, the fluid mesh is separated into two parts. The inner mesh moves with the rotor. The outer mesh keeps still. Then, the variable values are passed through the sliding interface. The complex re-meshing approach is implemented. For the traditional Arbitrary-Lagrangian-Eulerian method, the complicated re-meshing algorithm needs to be implemented.

CONCLUSION

In the present paper, the IVM is implemented to solve fluid structure interaction problems, where the solid is immersed in

the fluid domain as a finite volume. The ability to properly capture the dynamics of the solid and describe the flow distribution is verified by two cases. The major conclusions are as follows:

1. The fictitious fluid particles are introduced for mathematical purposes to satisfy the fluid-like equations in the whole domain, the velocity of which is independent of solid particles.
2. The velocity on the fictitious fluid-structure interface is determined by the nodal velocities on the real fluid-structure boundary and in the real fluid domain, which is independent of that in the fictitious fluid domain. The basic physical interpretation is satisfied and accuracy is preserved.
3. The FCBI finite element procedure is applied in fixed grid method for the first time. The FCBI scheme shows stabilities solving fluid-like equations with the external force.
4. The special feature of the proposed method assures its potential to solve incompressible fluid and compressible solid interaction problems, which greatly extend the application of the method.

ACKNOWLEDGMENTS

This work was supported by the Independent scientific research project of Tsinghua University(523014002).

REFERENCES

[1] Hirth, C. and Amsden, A. A., Cook, J., 1974. "An Arbitrary Lagrangian-Eulerian computing method for all flow speeds". *J. Comput. Phys, **14**, pp. 227-253.*

[2] Belytschko, T. and Kennedy, J. M., 1978, "Computer models for subassembly simulation". *Nucl Engrg Des, **49**, pp. 17-38*.

[3] Peskin, C. S., 1972, "Flow patterns around heart valves: a numerical method". *Journal of Computational Physics, **10**(2), pp. 252-271*.

[4] Lee, L. and LeVeque, R. J., 2003, :An immersed interface method for incompressible Navier-Stokes equations". *SIAM J Scientific Comput, **25** (3), pp. 832-856*.

[5] LeVeque, R.J. and Calhoun, D., 2001, *Cartesian grid methods for fluid flow in complex geometries*, Vol. 124. in: L.J. Fauci, S. Gueron (Eds.), Computational Modeling in Biological Fluid Dynamics, IMA Volumes in Mathematics and its Applications , Springer-Verlag.

[6] Peskin, C. S., 2002, "The immersed boundary method". *Acta Numer, **11**, pp. 479-517*.

[7] Xiaodong, W. and Wing K. L., 2004, "Extended immersed boundary method using FEM and RKPM". *Comput Methods Appl Mech Engrg, **193**, pp. 1305-1321*.

[8] Lucy Z., and Axel G., Xiaodong W., Wing K. L., 2004, "Immersed finite element method". *Comput Methods Appl Mech Engrg, **193**, pp. 2051-2067*.

[9] Wing, K. L., and Sukky, J., Yi, F. Z., 1995, "Reproducing kernel particle methods". *Int J Numer Methods Fluids, **20**, pp. 1081-1106*.

[10] Wing K. L., and Yaling L., David F., et al. 2006, "Immersed finite element method and its applications to biological systems". *Comput Methods Appl Mech Engrg, **195**, pp. 1722-1749*.

[11]Sylvain V., and Theodore P., 2010, "A trilinear immersed finite element method for solving the electroencephalography forward problem". *Society for Industrial and Applied Mathematics, **32**, pp. 2379-2394*.

[12]Gay M., and Zhang L., Liu, W. K., 2006, "Stent modeling using immersed finite element method". *Computer Methods in Applied Mechanics and Engineering, **195**, pp. 4358-4370*.

[13]Lee, T. R., and Chang, Y. S., Choi, J. B., et al. 2009, "Numerical Simulation of a Nanoparticle Focusing Lens in a Microfluidic Channel by Using Immersed Finite Element Method". *Journal of Nanoscience and Nanotechnology, **9**(12), pp. 7407-7411*.

[14]Lee, T. R., and Chang, Y. S., Choi, J. B., et al. 2008, "Immersed finite element method for rigid body motions in the incompressible Navier-Stokes flow". *Comput Methods Appl Mech Engrg, **197**, pp. 2305-2316*.

[15]Thomas, R., and Fehmi, C., 2011, "An immersed finite element method with integral equation correction". *International Journal for Numerical Methods in Engineering, **86**, pp. 93-114*.

[16]Xingshi, W., and Lucy, T. Z., 2013, "Modified immersed finite element method for fully-coupled fluid-structure interactions". *Computer Methods in Applied Mechanics and Engineering, **267**, pp. 150-169*.

[17]Bathe, K. J., 1996, "Finite Element Procedures". *Prentice-Hall: Englewood Cliffs, NJ*.

[18] Bathe, K. J., and Hou, Z., 2002, "A flow-condition-based interpolation finite element procedure for incompressible fluid flows". *Computers and Structures, **80**, pp. 1267-1277*.

[19] Bathe, K. J., and Hou, Z., 2004, "Finite element developments for general fluid flows with structure interactions". *Int J Numer Meth Engng, **60**, pp. 213-232*.

[20] Balaras, E., 2004, "Modeling complex boundaries using an external force field on fixed Cartesian grids in large-eddy simulations". *Computers & Fluids, **33**, pp. 375-404*.